# Novel Properties of the Wheat Aluminum Tolerance Organic Acid Transporter (TaALMT1) Revealed by Electrophysiological Characterization in *Xenopus* Oocytes: Functional and Structural Implications[1][OA]

**Miguel A. Piñeros, Geraldo M.A. Cançado[2], and Leon V. Kochian***

United States Plant, Soil, and Nutrition Laboratory, United States Department of Agriculture-Agricultural Research Service, Cornell University, Ithaca, New York 14853–2901 (M.A.P., L.V.K.); and Laboratório de Genômica Funcional, Centro de Biologia Molecular e Engenharia Genética, Universidade Estadual de Campinas, Campinas, São Paulo, Brazil 13083–970 (G.M.A.C.)

Many plant species avoid the phytotoxic effects of aluminum (Al) by exuding dicarboxylic and tricarboxylic acids that chelate and immobilize $Al^{3+}$ at the root surface, thus preventing it from entering root cells. Several novel genes that encode membrane transporters from the ALMT and MATE families recently were cloned and implicated in mediating the organic acid transport underlying this Al tolerance response. Given our limited understanding of the functional properties of ALMTs, in this study a detailed characterization of the transport properties of TaALMT1 (formerly named ALMT1) from wheat (*Triticum aestivum*) expressed in *Xenopus laevis* oocytes was conducted. The electrophysiological findings are as follows. Although the activity of TaALMT1 is highly dependent on the presence of extracellular $Al^{3+}$ ($K_{m1/2}$ of approximately 5 $\mu$M $Al^{3+}$ activity), TaALMT1 is functionally active and can mediate ion transport in the absence of extracellular $Al^{3+}$. The lack of change in the reversal potential ($E_{rev}$) upon exposure to $Al^{3+}$ suggests that the "enhancement" of TaALMT1 malate transport by Al is not due to alteration in the transporter's selectivity properties but is solely due to increases in its anion permeability. The consistent shift in the direction of the $E_{rev}$ as the intracellular malate activity increases indicates that TaALMT1 is selective for the transport of malate over other anions. The estimated permeability ratio between malate and chloride varied between 1 and 30. However, the complex behavior of the $E_{rev}$ as the extracellular $Cl^-$ activity was varied indicates that this estimate can only be used as a general guide to understanding the relative affinity of TaALMT1 for malate, representing only an approximation of those expected under physiologically relevant ionic conditions. TaALMT1 can also mediate a large anion influx (i.e. outward currents). TaALMT1 is permeable not only to malate but also to other physiologically relevant anions such as $Cl^-$, $NO_3^-$, and $SO_4^{2-}$ (to a lesser degree).

Plant species have evolved diverse mechanisms that enable them to overcome the phytotoxic effects of aluminum ($Al^{3+}$) commonly found in acidic soils (for recent reviews, see Kochian et al., 2004, 2005). The most compelling experimental evidence indicates that several monocot and dicot plant species exclude $Al^{3+}$ from entering the cells of the root tip by exuding dicarboxylic and tricarboxylic acids (e.g. citrate, malate, and/or oxalate) and immobilizing $Al^{3+}$ at the root surface by forming stable, nontoxic complexes. The original reports in wheat (*Triticum aestivum*; Delhaize et al., 1993a, 1993b) showing that Al-activated malate release correlates with differential Al tolerance are seminal studies for the subsequent numerous publications showing that Al-activated organic acid release correlates with the Al tolerance observed in many other plant species (see table I in Kochian et al., 2004). Subsequent to these initial studies, there have been several publications aimed at identifying potential candidates for the membrane transporters mediating these Al-activated processes. The thermodynamic nature of organic acid efflux suggests the presence of a large outwardly directed gradient (i.e. from the cytosol to the extracellular space) due to the speciation of organic acids as organic anions in the cytosol, with their passive efflux driven by the negative transmembrane electrical potential. Consequently, anion channels were identified as plausible candidates, as they could mediate the transport of these organic anions down their electrochemical gradient (i.e. efflux). This realization resulted in the implementation of electro-

[1] This work was supported by the U. S. Department of Agriculture National Research Initiative (Plant Biology: Environmental Stress grant no. 2007–35100–18436), by the National Science Foundation (Plant Genome grant no. DBI 0419435), and by Generation Challenge (grant no. IC69). G.M.A.C. was supported by scholarships from Fundação de Amparo à Pesquisa do Estado de Minas Gerais and Coordenação de Aperfeiçoamento de Pessoal de Nível Superior.

[2] Present address: Empresa de Pesquisa Agropecuária de Minas Gerais, Belo Horizonte, Brazil 31170–000.

* Corresponding author; e-mail lvk1@cornell.edu.

The author responsible for distribution of materials integral to the findings presented in this article in accordance with the policy described in the Instructions for Authors (www.plantphysiol.org) is: Leon V. Kochian (lvk1@cornell.edu).

[OA] Open Access articles can be viewed online without a subscription.

www.plantphysiol.org/cgi/doi/10.1104/pp.108.119636

physiological approaches to study these processes, which led to the discovery and characterization of plasma membrane anion channel-mediated currents, which were specifically activated by extracellular $Al^{3+}$. These studies performed in protoplasts isolated from root tips of Al-resistant wheat (Ryan et al., 1997; Zhang et al., 2001) and maize (*Zea mays*; Kollmeier et al., 2001; Piñeros and Kochian, 2001; Piñeros et al., 2002) showed remarkable similarities between the transport and activation properties of these channels and the Al-activated malate and citrate exudation responses reported in intact wheat and maize roots, suggesting that these types of transporters are likely to mediate the Al-activated organic acid release observed at the whole root level.

More recently, *TaALMT1* (formerly named *ALMT1*), a gene encoding a novel Al-activated malate transporter, was cloned from wheat (*Triticum aestivum*; Sasaki et al., 2004) and then subsequently shown to confer increased Al tolerance in roots of transgenic barley (*Hordeum vulgare*) plants (Delhaize et al., 2004). Functional studies in *Xenopus laevis* oocytes suggested that TaALMT1 was activated in the presence of extracellular $Al^{3+}$ and was permeable to malate. This discovery, in conjunction with the plasma membrane localization of this protein (Yamaguchi et al., 2005), its expression profile, and genetic and physical mapping to the same region in the wheat genome as the major Al tolerance locus (Raman et al., 2005), strongly suggest that *TaALMT1* is a major Al tolerance gene in wheat, possibly encoding the $Al^{3+}$-activated transporter previously characterized electrophysiologically in protoplasts of Al-tolerant wheat lines. Subsequently, studies in Arabidopsis (*Arabidopsis thaliana*) and rape (*Brassica napus*) have identified TaALMT1 homologues from other plant species. For example, the Arabidopsis (*AtALMT1*) and rape (*BnALMT1* and *BnALMT2*) homologues were also shown to encode Al-activated malate transporters that mediate Al-activated malate exudation in roots, which is critical for Al tolerance and possibly underlying the Al tolerance response in these plant species (Hoekenga et al., 2006; Ligaba et al., 2006). The biochemistry and genetics of the ALMT family, and their involvement (as inferred from the functional data available to date) in mediating the $Al^{3+}$ tolerance mechanisms based on organic anion efflux, were recently reviewed (Delhaize et al., 2007). Interestingly, the transport characteristics for the most recently cloned ALMT1 homologue from maize (*ZmALMT1*) suggest that this transporter is not likely to mediate Al-activated citrate exudation in maize roots and is not involved in Al tolerance (Piñeros et al., 2008). Regardless of the high sequence identity between ZmALMT1 and all other ALMT1 homologues characterized so far, ZmALMT1 encodes a protein that, although it mediates anion-selective transport, shows poor permeability/selectivity for organic anions relative to other anions such as $Cl^-$. Likewise, ZmALMT1 activity is only very weakly enhanced by extracellular $Al^{3+}$. This discovery, in conjunction with the large diversity of ALMT-type transporters found in the Aromatic Acid Efflux family, is not surprising, as new members of this family are starting to emerge with new functional properties and different roles from those originally assigned in terms of $Al^{3+}$ tolerance. For example, recently, the Arabidopsis homologue *AtALMT9* was shown to encode a vacuolar malate anion channel (Kovermann et al., 2007). In addition, members of a different family of transporters have also been shown to be involved in the Al-activated organic acid response. Al tolerance in sorghum (*Sorghum bicolor*) was recently shown to be determined by $Alt_{Sb}$, a gene encoding a member of the multidrug and toxin efflux (MATE) protein family, which confers sorghum Al tolerance via the mediation of Al-activated root citrate efflux (Magalhaes et al., 2007).

Although reports on an increasing number of ALMT-type transporters that possibly underlie the Al tolerance response in plant species are starting to emerge, very little is known regarding the specific biophysical properties of these ALMTs that confer diverse physiological functions in both mineral nutrition and abiotic stress tolerance. Thus, there is an immediate need to understand the biophysical and electrophysiological bases of the ion transport mediated by these proteins in order to provide a framework to link their structural and functional properties to specific functions in the plant. This study greatly expands the preliminary characterization of TaALMT1 from wheat first reported by Sasaki et al. (2004) by thoroughly characterizing its biophysical properties in *Xenopus* oocytes and by beginning to provide an understanding of the relationship between the structure and the function of this transporter.

## RESULTS

The initial electrophysiological characterization of TaALMT1 expressed in *Xenopus* oocytes was performed under identical extracellular ionic conditions (i.e. ND88 solution) to those originally reported by Sasaki and coworkers (2004). Subsequently, the biophysical properties of TaALMT1 were studied in a range of different ionic environments, which helped elucidate several of its transport properties (see Tables I and II for complete descriptions of the bath solutions used). Figure 1 depicts the basic biophysical characteristics of TaALMT1 recorded in ND88 bath solution. Figure 1A illustrates the time course of activation of an inward current in TaALMT1-expressing cells as the bath solution was replaced by an identical solution containing 100 $\mu$M $AlCl_3$ (8 $\mu$M $Al^{3+}$ activity). The activation response showed a lag in time (about 2 min) between the initiation of the perfusion and the complete activation of the current, presumably reflecting the time required for the new ionic environment to reach equilibrium with the plasma membrane across the vitelline envelope surrounding the cell. In contrast, exposure to $Al^{3+}$ did not activate any endogenous

**Table I.** *Ionic composition (in mM) of bath solutions*

The pH of all solutions (with or without 0.1 $AlCl_3$) was adjusted to 4.5.

| Solution | Ionic Composition | | | | | | | | | |
|---|---|---|---|---|---|---|---|---|---|---|
| | $Cl^-$ | $NO_3^-$ | $SO_4^{2-}$ | $Na^+$ | Choline | MES | $K^+$ | $Ca^{2+}$ | $Mg^{2+}$ | $La^{3+a}$ |
| Ringer (ND88) | 105.0 | 12.4 | 0.8 | 90.4 | − | − | 1 | 20.9 | 0.8 | − |
| ND96 | 101.6 | − | − | 96.0 | − | − | 2 | 1.8 | − | −/+ |
| Choline chloride | 101.6 | − | − | − | 96 | − | 2 | 1.8 | − | + |
| MES | 3.6 | − | − | − | − | 96 | 2 | 1.8 | − | + |

[a]Where indicated, $La^{3+}$ was present at 0.1 mM.

inward currents in control cells (i.e. nonexpressing). Figure 1, B and C, shows the steady-state currents and the current-to-voltage relationship (I/V) obtained for control and TaALMT1-expressing cells prior to and following the addition of $Al^{3+}$ to the ND88 bath medium. Exposure to $Al^{3+}$ resulted in the activation of large inward and outward currents in TaALMT1-expressing cells relative to those recorded in control cells. In contrast, exposure to $Al^{3+}$ resulted in a slight inhibition of the already considerably smaller *Xenopus* oocyte endogenous inward and outward currents recorded in control cells. It is important to mention that in most batches of cells, voltage pulses more negative than −100 mV did not activate any of the large endogenous inward currents frequently reported in *Xenopus* oocytes. As the I/V relationships described in this study were obtained over a wide range of holding potentials, these data uncovered new transport features in addition to the basic transport features originally described for TaALMT1 (Sasaki et al., 2004). These new findings include the following. (1) In the absence of extracellular $Al^{3+}$, TaALMT1-expressing and control cells showed no significant differences in the magnitude of the inward current at holding potentials less negative than −90 mV. However, at holding potentials more negative than −100 mV, TaALMT1-expressing cells mediated significantly larger negative currents than control cells (Fig. 1, B and C). These observations suggest that TaALMT1 is functionally active and mediates ion transport even in the absence of extracellular $Al^{3+}$. (2) At holding potentials more positive than + 50 mV, TaALMT1-expressing cells showed significantly larger positive current (i.e. outward current due to either anion influx or cation efflux) relative to the control cells (Fig. 1, B and C). The outward currents recorded in TaALMT1-expressing cells were significantly larger and had quite different current kinetics than the endogenous currents recorded in control cells. The endogenous outward currents recorded in control cells (Fig. 1B, left) were dominated by time-dependent currents that activated slowly and were attenuated by the presence of $Al^{3+}$ in the bath medium. In contrast, the outward currents in TaALMT1-expressing cell were dominated by large, instantaneously activated currents and were significantly enhanced by the presence of extracellular $Al^{3+}$ (Fig. 1B, right). The instantaneous nature of the TaALMT1-mediated outward currents was more evident at holding potentials more positive than +60 mV, as the contribution (i.e. magnitude) of the TaALMT1-mediated currents became significantly larger relative to the endogenous time-dependent background currents at large (>60 mV) positive potentials. Figure 1D shows the resulting current kinetics (traces) and I/V relationship expected for the net $Al^{3+}$-enhanced TaALMT1 obtained by subtracting the endogenous currents from those recorded in TaALMT1-expressing cells. Overall, these data indicate that the kinetics for both TaALMT1-mediated inward and outward currents are dominated by instantaneously activated kinetics.

In order to gain a better understanding of the nature and identity of the TaALMT1-mediated currents, the extracellular ionic conditions were systematically exchanged (see Tables I and II for the detailed ion compositions of all solutions). We first modified the original ND88 bath solution by removing $NO_3^-$ and $SO_4^{2-}$ and substantially decreasing the $Ca^{2+}$ concentration, with the main purpose of having $Cl^-$ as the only anion present in the bath solution (i.e. ND96 solution). Under this set of ionic conditions, we proceeded to examine the specificity and affinity by which $Al^{3+}$ enhances the activity of TaALMT1 by characterizing the effects of different lanthanides on

**Table II.** *Ionic composition (in mM) of bath solutions in which $Cl^-$ was varied by decreasing the NaCl concentration (as indicated by the ND suffix)*

The Al concentrations used to maintain a constant $Al^{3+}$ activity of 10 μM through the solutions are indicated in the fourth column. The fifth column indicates the predicted $Cl^-$ activity ($\{Cl^-\}_o$). Ionic activities were calculated using the GEOCHEM speciation program. All solutions contained 1 mM KCl, 1.8 mM $CaCl_2$, and 0.1 mM $LaCl_3$ in the background. The osmolarity of all solutions was adjusted to 195 mosmol with sorbitol, and the pH was adjusted to 4.5.

| Solution | Ionic Composition | | | |
|---|---|---|---|---|
| | $Na^+$ | $Cl^-$ | $AlCl_3$ | $\{Cl^-\}_o$ |
| ND96 | 96 | 101 | 0.10 | 75 |
| ND72 | 72 | 77 | 0.08 | 59 |
| ND48 | 48 | 53 | 0.06 | 41 |
| ND24 | 24 | 29 | 0.05 | 24 |
| ND15 | 15 | 20 | 0.04 | 14 |
| ND0 | 0 | 5 | 0.02 | 5 |

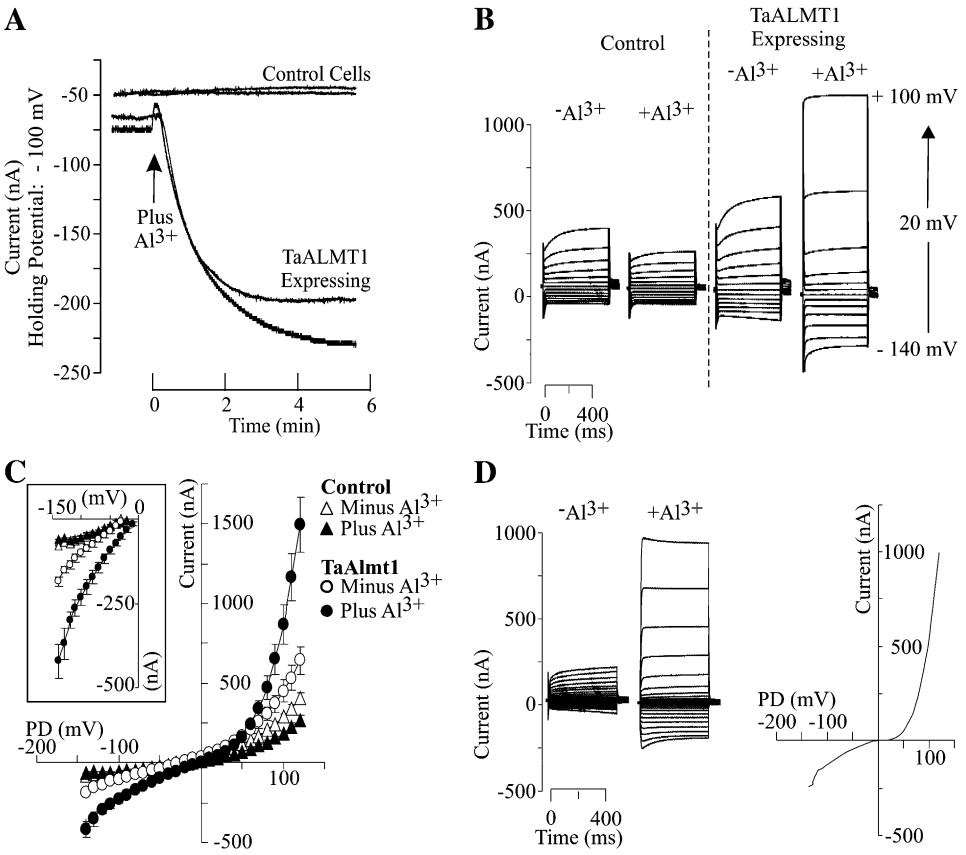


**Figure 1.** Electrophysiological characterization of TaALMT1-expressing and control (i.e. not injected with cRNA) *Xenopus* oocytes preloaded with malate. A, Extracellular $Al^{3+}$ induces an inward current in oocytes expressing TaALMT1. Net currents were recorded at −100 mV. The arrow indicates the time point when the ND88 bath solution (see "Materials and Methods" for detailed composition) was exchanged by ND88 solution containing 100 $\mu$M $AlCl_3$ (8 $\mu$M $Al^{3+}$ activity). Cells were preloaded with malate, yielding an intracellular malate concentration of approximately 8 mM (4.5 mM $mal^{2-}$ activity; see "Materials and Methods" for loading protocols and cytoplasmic malate determinations). Each trace was recorded from a different cell. B, Examples of families of currents from control and TaALMT1-expressing cells recorded in ND88 solution lacking or containing 100 $\mu$M $AlCl_3$ (8 $\mu$M $Al^{3+}$ activity) in response to voltage pulses ranging from −140 to +100 mV in 20-mV steps (see "Materials and Methods" for detailed protocol). C, Mean I/V relationships from control (triangles) and TaALMT1-expressing (circles) oocytes recorded in the absence (white symbols) or presence (black symbols) of 100 $\mu$M $AlCl_3$ in ND88 solutions ($n$ = 14). The inset highlights the inward (i.e. negative) currents. D, Left, Examples of the net TaALMT1 currents. The resulting traces were obtained by subtracting the control cell current traces from recordings for the TaALMT1-expressing cells. These recordings were obtained in ND88 solution containing 100 $\mu$M $AlCl_3$ (8 $\mu$M $Al^{3+}$ activity) in response to voltage pulses ranging from −140 to +100 mV in 10-mV steps. Right, I/V relationship corresponding to the net $Al^{3+}$-enhanced TaALMT1-mediated current calculated by subtracting the background endogenous currents recorded from control cells (in the presence of $Al^{3+}$) from those recorded from TaALMT1-expressing cells in the presence of $Al^{3+}$. The net current was calculated from the average currents from the relationships shown in C.

the TaALMT1-mediated and endogenous (i.e. control) currents (Fig. 2). Figure 2A illustrates a long-term recording (up to 40 min long) of the TaALMT1-mediated inward current. Following the activation of the transporter by extracellular $Al^{3+}$, TaALMT1 does not undergo any inactivation provided that $Al^{3+}$ is present in the extracellular medium (Fig. 2A, trace 1). The reduction in current magnitude observed over this time period is due to a reduction of the electrochemical gradient across the membrane; that is, the chemical gradient for malate is collapsing as the intracellular malate source provided via microinjection of malate is depleted due to malate efflux over time. In contrast, no inward currents were activated in control cells exposed to $Al^{3+}$ over these longer time periods. The specificity of the response was examined by evaluating the effectiveness of lanthanides in maintaining the TaALMT1 activation response. Once activated by $Al^{3+}$, replacement of $Al^{3+}$ in the extracellular solution by a solution containing $La^{3+}$ or $Gd^{3+}$ was ineffective at maintaining the activation of the TaALMT1-mediated inward current, resulting in current inactivation (Fig. 2A, trace 2). Replacement of $La^{3+}$ or $Gd^{3+}$ by $Al^{3+}$ resulted in full reactivation of the transporter. Likewise, TaALMT1-expressing cells that had not been preloaded with malate (Fig. 2A, trace 3) showed a similar

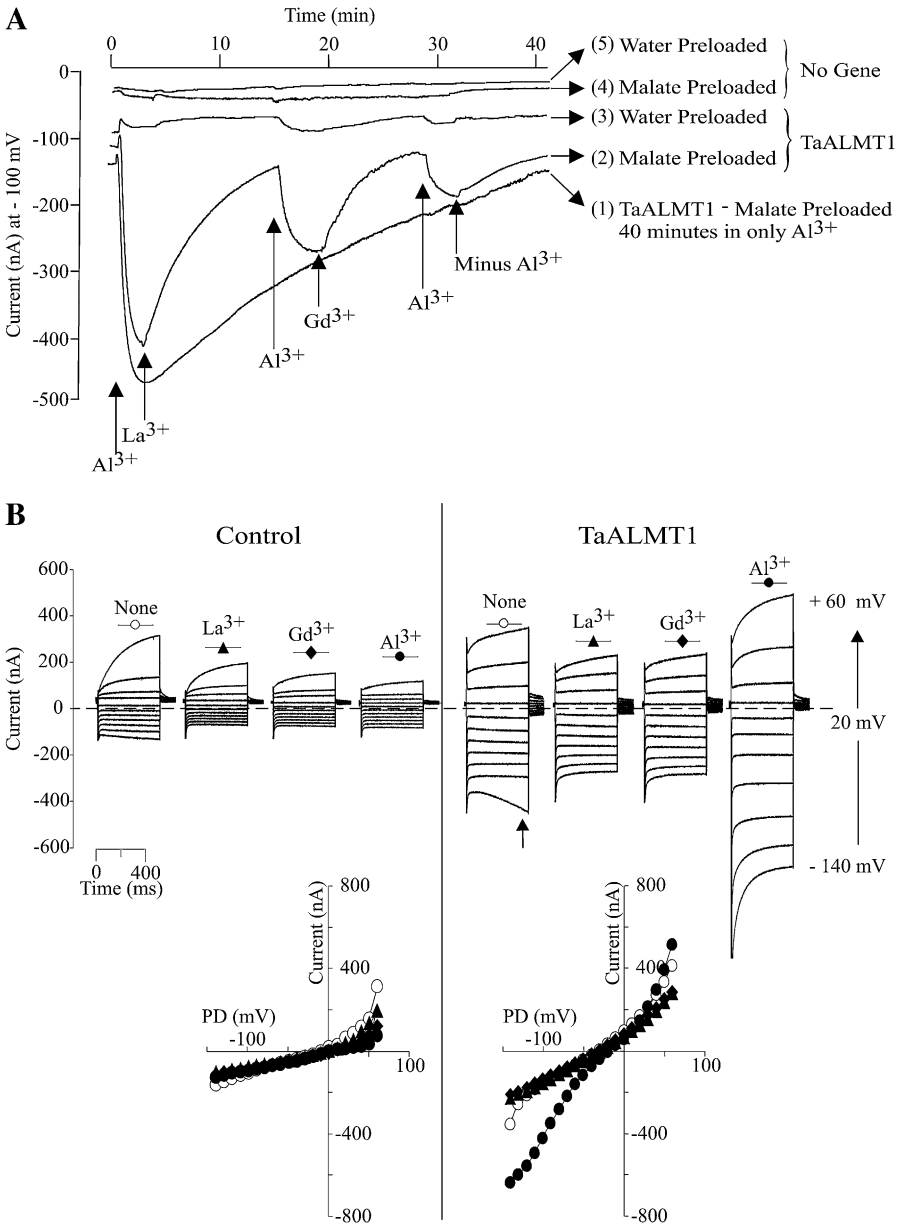


**Figure 2.** Cation specificity of TaALMT1 activation by extracellular $Al^{3+}$. A, Extracellular $Al^{3+}$ is required to maintain TaALMT1 activation. Trace 1 shows the TaALMT1-mediated inward current activity over a 40-min period following activation by $Al^{3+}$ (100 $\mu$M $AlCl_3$ concentration at the time indicated by the arrow) in a malate-preloaded cell. Traces 2 and 3 show the activity of the TaALMT1 inward current in malate-preloaded (trace 2) or water-preloaded (trace 3) cells following activation by $Al^{3+}$ and subsequent exchange of solutions containing 100 $\mu$M of the trivalent cations indicated at the bottom of the traces. Recordings from control cells preloaded with malate or water and subjected to identical treatments as those shown for traces 2 and 3 are shown for reference (traces 4 and 5, respectively). All traces were taken from different cells bathed in ND96 solution. Similar responses were observed for at least three other cells for each case and ionic condition. B, Examples of families of currents recorded from control (left) and TaALMT1-expressing (right) cells preloaded with malate and bathed in ND96 solution containing 100 $\mu$M lanthanide (described at the top of each set of traces). Currents shown are in response to voltage pulses ranging from −140 to +60 mV. The arrow in the right panel indicates the endogenous time-dependent inward currents recorded at large negative potentials occasionally detected in some cell batches. Note that the presence of this endogenous current was only evident when $Al^{3+}$ or analog lanthanides were not present in the bath solution. Similar recordings were observed in a total of six control and six TaALMT1-expressing cells tested. The bottom panel shows the I/V relationships obtained from the above recordings, with the symbols corresponding to those shown at the top of each set of traces.

pattern of inward current activation exclusively in the presence of extracellular $Al^{3+}$. However, the magnitude of the $Al^{3+}$-enhanced currents from nonpreloaded TaALMT1-expressing cells was significantly smaller. These results suggest that an endogenous intracellular substrate present in oocyte cells can also permeate via TaALMT1. We found the endogenous intracellular malate level to be approximately 0.2 mM; hence, it is possible that these small Al-activated inward currents in cells not loaded with malate are due to malate coming from the endogenous cytoplasmic pool. None of the $Al^{3+}$ specificity responses described above for TaALMT1-expressing cells were observed in control cells preloaded or not preloaded with malate (Fig. 2A, traces 4 and 5). Figure 2B shows examples of the steady-state currents recorded for control and TaALMT1-expressing cells under the same set of ionic conditions used for the data in Figure 2A.

The overall biophysical characteristics (i.e. kinetics) of the currents recorded for control and TaALMT1-expressing cells in ND96 solutions resembled those reported earlier in ND88 bath solutions. Exposure to 100 $\mu$M of any of the three lanthanides resulted in attenuation (i.e. partial blockade) of the endogenous inward and outward currents recorded in control cells (Fig. 2B, left). Addition of $La^{3+}$ or $Gd^{3+}$ to the bath solution did not lead to current activation in TaALMT1-expressing cells over the entire range of voltage pulses tested (Fig. 2B, right). Instead, the presence of $La^{3+}$ or $Gd^{3+}$ resulted in a minor attenuation of the outward (and to a lesser extent the inward) currents in TaALMT1-expressing cells, presumably

due to the blockade of endogenous transporters, similar to that observed in control cells. Overall, the currents recorded in TaALMT1-expressing cells in the presence of $La^{3+}$ or $Gd^{3+}$ resembled those recorded in the absence of lanthanides. In contrast, addition of $Al^{3+}$ to the bath medium resulted in the activation of significantly larger inward and outward TaALMT1-mediated currents relative to those recorded in control cells. It is worth noting that the kinetics of the outward currents from TaALMT1-expressing cells illustrated in Figure 2B (left) show a significant time-dependent component, presumably from the endogenous time-dependent outward currents, which were not entirely attenuated even in the presence of $Al^{3+}$ in the bath medium. As mentioned above, the contribution of the endogenous currents to the overall magnitude and kinetics of the TaALMT1-mediated outward currents becomes less significant at holding potentials more positive than + 60 mV, where the magnitude (i.e. conductance) and kinetics (i.e. instantaneous nature) are dominated by the TaALMT1-mediated currents relative to the small background endogenous time-dependent currents. Likewise, in the absence of $Al^{3+}$ or analog lanthanides, we could occasionally detect significantly large endogenous time-dependent inward currents at the most negative potentials in some batches of cells (as depicted by the arrow in the first set of traces in Fig. 2B, right [i.e. in the absence of extracellular lanthanides]). However, most batches of control and TaALMT1-expressing cells examined did not show activation of this endogenous current. Furthermore, these endogenous currents were effectively blocked by the presence of extracellular $La^{3+}$ or $Gd^{3+}$ (similar to the $Al^{3+}$ blockade of the endogenous inward and outward currents described in control cells in Fig. 1B). The blockade of endogenous currents by lanthanides described above is in agreement with other studies reporting irreversible inhibition of endogenous cation- and anion-mediated currents (e.g. hyperpolarization-activated $Cl^-$ channels [$Cl^-_{hyp}$] and volume-sensitive $Cl^-$ channels [$Cl^-_{vol}$] by lanthanides such as $La^{3+}$ or $Gd^{3+}$; Weber, 1999). Consequently, the net TaALMT1-mediated current in oocytes should be the product of the $Al^{3+}$ enhanced, TaALMT1-mediated currents minus the endogenous currents that remain following inhibition of a significant portion of the endogenous currents by lanthanides (both inhibitions caused by $Al^{3+}$ and $La^{3+}$). We took advantage of the differences between the unique properties of TaALMT1 activation and the pharmacological profile of the endogenous currents (i.e. $La^{3+}$ effectively blocks endogenous currents but does not activate the TaALMT1-mediated currents) to characterize the affinity of TaALMT1 for $Al^{3+}$ in bath solutions containing $La^{3+}$ in the background (i.e. ND96LA). The I/V relationships in Figure 3 illustrate the enhancement of the net TaALMT1-mediated inward currents as the extracellular $Al^{3+}$ activities were increased from 0 to 19 $\mu$M. The current enhancement at a given $Al^{3+}$ activity was significantly higher at more negative holding potentials. Figure 3B illustrates the $Al^{3+}$ activity-dependent enhancement of the net TaALMT1-mediated inward conductance, resulting in a $K_{m1/2}$ of about 5 $\mu$M $Al^{3+}$ activity.

We proceeded to investigate the nature of the TaALMT1-mediated inward current. The assumption that malate efflux underlies the inward current mediated by TaALMT1 was originally based solely on the observation that the conductivity of the $Al^{3+}$-activated inward current in malate/citrate-preloaded *Xenopus* oocytes expressing TaALMT1 was significantly larger than in cells not preloaded with the organic acid. The observed increase in conductivity was presumably due to an increase in membrane permeability (i.e. transport) via TaALMT1. In order to verify this assumption and provide irrefutable evidence that permeation of malate via TaALMT1 takes place in a selective manner, we compared the TaALMT1-mediated currents from cells that were preloaded with malate with those from cells preloaded with water. Figure 4A illustrates the I/V relationships obtained for these cells (and their respective controls) bathed in ND96LA solution prior to and following the addition of 10 $\mu$M $Al^{3+}$ activity. TaALMT1-expressing cells preloaded with water exhibited similar transport features to oocytes preloaded with malate. These features include the following: (1) at extreme negative and positive potentials, TaALMT1-expressing cells mediate significantly larger negative and positive currents than control cells, even in the absence of extracellular $Al^{3+}$ (Fig. 4A, right), and (2) TaALMT1-mediated currents in these cells were also enhanced in the presence of $Al^{3+}$. These results indicate that TaALMT1 is functionally active and mediates ion transport regardless of the presence of extracellular $Al^{3+}$ and the presence of internal malate (i.e. in cells preloaded with malate). Figure 4B illustrates the TaALMT1-specific inward currents calculated by subtracting the control cell currents measured in identical ionic conditions (i.e. the absence and presence of $Al^{3+}$). In the absence of extracellular $Al^{3+}$, TaALMT1-expressing cells that had been preloaded with malate mediated inward currents, which were significantly enhanced upon the addition of $Al^{3+}$ to the bath medium. The reversal potential ($E_{rev}$) of the TaALMT1-mediated currents from cells preloaded with malate remained unchanged at about −12 mV upon addition of $Al^{3+}$. This result suggests that enhancement of TaALMT1 activity by $Al^{3+}$ (presumably the binding of $Al^{3+}$ to the protein) results in a change of its absolute permeability but not its selectivity. Similar results were recorded for TaALMT1-expressing cells that were preloaded with water, where upon exposure to $Al^{3+}$ the $E_{rev}$ remained unchanged at about −30 mV. Interestingly, the $E_{rev}$ value of the cells preloaded with water was significantly more negative than in cells preloaded with malate. Figure 4C highlights the positive shift in the $E_{rev}$ (about +18 mV) as the intracellular malate activity was increased by preloading the cells with about 8 mM malate (i.e. 4.5 mM $mal^{2-}$ activity; see "Materials and Methods" for

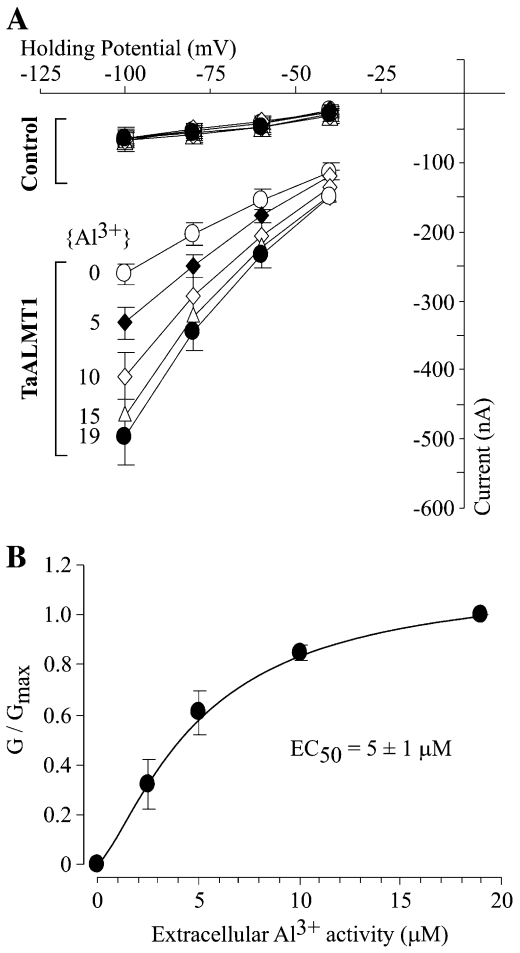


**Figure 3.** Affinity of TaALMT1 for $Al^{3+}$ as demonstrated by the relationship between the magnitude of the TaALMT1-mediated inward current and the extracellular $Al^{3+}$ activity present in ND96LA bath medium (ND96 containing 100 $\mu$M $LaCl_3$). A, I/V relationship obtained for control and TaALMT1-expressing cells preloaded with malate and bathed in ND96LA solution plus $Al^{3+}$ (activities from 0 to 19 $\mu$M $Al^{3+}$; $n = 6$). B, Normalized conductances were calculated as the ratio of the corrected conductance ($G_{\text{in the presence of Al3+}} - G_{\text{in the absence of Al3+}}$) and the maximum conductance (at 19 $\mu$M $Al^{3+}$) plotted against the extracellular $Al^{3+}$ activity and fitted to the Hill equation: $G = G_{max}/(EC_{50}{}^{n}/[Al^{3+}]^{n} + 1)$, where $n$ is the Hill coefficient, $EC_{50}$ is the concentration of half enhancement, and $G_{max}$ is the corrected maximum conductance. Best fitting resulted in $G_{max} = 1.1 \pm 0.1$, $EC_{50} = 5 \pm 1$ $\mu$M $Al^{3+}$, and a Hill coefficient of $n = 1.4 \pm 0.4$ ($r^2 = 0.993$). Values represent averages of at least six different TaALMT1-expressing and control cells.

intracellular malate determinations). The direction of this shift is consistent with malate being the anion underlying the TaALMT1 inward current (i.e. malate efflux). On the other hand, the strong outwardly directed malate gradient (due to the lack of malate in the extracellular bath solution) results in a theoretical equilibrium potential ($E_{mal}{}^{2-}$) for malate that is infinitely positive. Nonetheless, the $E_{rev}$ values recorded in TaALMT1-expressing cells were significantly more negative (−12 to −30 mV) than $E_{mal}{}^{2-}$. This indicates that other ion(s) also permeate TaALMT1 and contribute to the $E_{rev}$ recorded. Likewise, the presence of a small TaALMT1-mediated $Al^{3+}$-activated inward (i.e. negative) current recorded in cells in which malate was not preloaded (i.e. water-injected cells) is in agreement with the idea that TaALMT1 is also permeable to an unknown endogenous anion. Finally, it is worth highlighting the presence of some experimental variability in the magnitude of the TaALMT1-mediated currents between this specific batch of cells (Fig. 4) and those shown in the previous figures. Rather than normalizing the currents, the electrogenic activity of each batch of control cells in each ionic condition is presented, to allow the comparison between TaALMT1-expressing and control cells within each data set. Similar controls were performed throughout the remainder of the study.

To further address the permeability and selectivity properties of TaALMT1-mediated inward current, the next batch of cells was used to examine the $Na^+$ dependence of TaALMT1-mediated transport by replacing sodium chloride with choline chloride in the bath medium (Fig. 5). In the absence of extracellular $Na^+$, the permeability and regulatory properties of TaALMT1 were not altered. The TaALMT1-mediated inward current exhibited similar $E_{rev}$ values in the presence and absence of $Na^+$. The presence or absence of $Na^+$ also had no effect on the current enhancement mediated by exposure to $Al^{3+}$. Furthermore, preloading the cells with malate resulted both in a similar increase in the magnitude of the TaALMT1-mediated inward currents and in a positive shift in $E_{rev}$ (about +18 mV), independent of $Na^+$ conditions. These results indicate that TaALMT1 transport exhibits high anion selectivity relative to $Na^+$.

The next set of ionic conditions was designed to investigate the dependence of the TaALMT1-mediated inward current on the nature of the extracellular anion environment. Extracellular $Cl^-$ (the only anion present in the bath medium) was minimized by replacing the NaCl in the bath solution by MES (Table I). The latter has been shown to attenuate the major hyperpolarization-induced and volume-sensitive endogenous chloride currents in oocytes (Mitcheson et al., 2000). In the absence of lanthanides, replacement of NaCl by MES effectively inhibited the predominant endogenous time-dependent outward currents in control cells (Fig. 6A, left). Figure 6A, right, illustrates an example of current traces recorded in TaALMT1-expressing cells preloaded with malate and bathed in MES solution in the absence and presence of extracellular $Al^{3+}$. Figure 6B shows the average steady-state I/V relationships obtained for control and TaALMT1-expressing (both malate- and water-preloaded) cells prior to and following the addition of $Al^{3+}$ to the MES-containing bath medium. TaALMT1-expressing cells displayed permeability and regulatory properties similar to those described for the previous ionic environments (inward currents that were enhanced upon exposure to $Al^{3+}$). The presence of significant TaALMT1-mediated inward

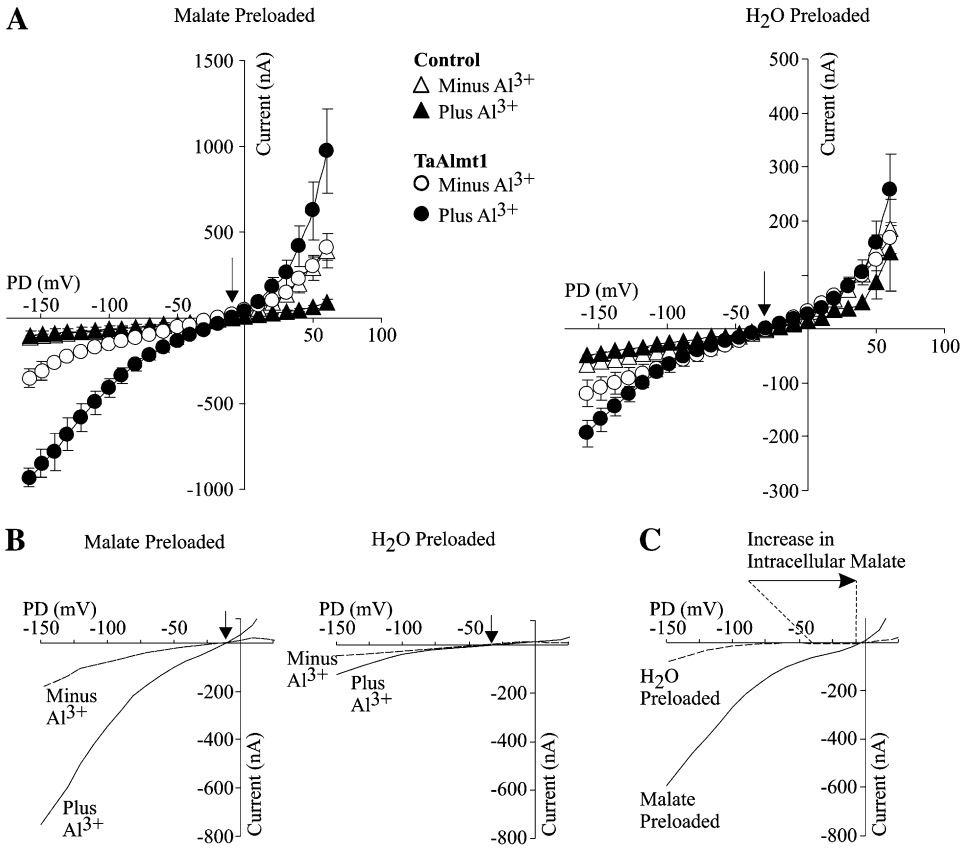


**Figure 4.** Malate efflux underlies the inward TaALMT1-mediated current. A, Mean I/V relationships obtained in TaALMT1-expressing (circles) and control (triangles) cells preloaded with malate (left) or water (right). Recordings were performed in ND96LA solution minus (white symbols) or plus (black symbols) 10 $\mu$M $Al^{3+}$ activity ($n$ = 10). Malate preloading resulted in an internal malate concentration increase of 8.2 mM compared with the 200 to 400 $\mu$M endogenous malate present in water-injected cells (see "Materials and Methods" for internal malate determinations). Note the different current scales between the two panels ($n$ = 16). B, Net inward TaALMT1-mediated current obtained after subtraction of the endogenous currents recorded in control cells. The I/V relationships illustrate the magnitude and the $E_{rev}$ (arrows) of the inward currents in cells preloaded with malate (left) or water (right) prior to (dashed line) and after (solid line) exposure to extracellular $Al^{3+}$. C, Preloading cells with malate led to an increase in the magnitude of the TaALMT1-mediated inward current and a shift in $E_{rev}$ (arrow and dotted lines) to more positive potentials. The I/V relationship shown corresponds to the net enhanced TaALMT1 mediated current corresponding to the difference between the current in the presence and absence of $Al^{3+}$, calculated after subtracting the endogenous currents recorded in control cells. Currents were calculated from the relationships shown in A.

currents in water-injected cells corroborated that TaALMT1 can also mediate the efflux of an unknown endogenous substrate (which may be endogenous malate). Increasing the internal concentration of malate also resulted in a positive shift in $E_{rev}$ (from +20 to +55 mV), corroborating earlier observations that malate underlies the TaALMT1 inward current (i.e. malate efflux). However, the $E_{rev}$ values from water- and malate-preloaded cells bathed in MES solution were significantly more positive than those recorded in bath solutions containing higher levels of $Cl^-$ (i.e. ND96LA and choline chloride). Likewise, the magnitude of the shift in $E_{rev}$ recorded in MES bath solutions (about +35 mV) upon increasing the intracellular malate concentration was significantly larger than in bath solutions containing higher $Cl^-$ concentrations (about +18 mV in ND96LA and choline chloride). These results indicate that the $E_{rev}$ recorded in TaALMT1-expressing cells is not only dependent on the internal malate concentration but is also dependent on extracellular $Cl^-$.

The analysis of the I/V relationships obtained in MES solution did not show any signs of a significant TaALMT1-mediated outward current at holding potentials more positive than the $E_{rev}$ (Fig. 6), in contrast to the I/V relationships obtained in ND88 (Fig. 1), ND96La (Fig. 4), or choline chloride (Fig. 5) bath solutions. Consequently, the next set of experiments was aimed at examining the nature of the TaALMT1-mediated outward current and characterizing the anion selectivity of TaALMT1. This was accomplished by examining the I/V relationships of malate- or water-preloaded cells as the extracellular $Cl^-$ activity ($\{Cl^-\}_o$) was varied while maintaining the $Al^{3+}$ activity constant

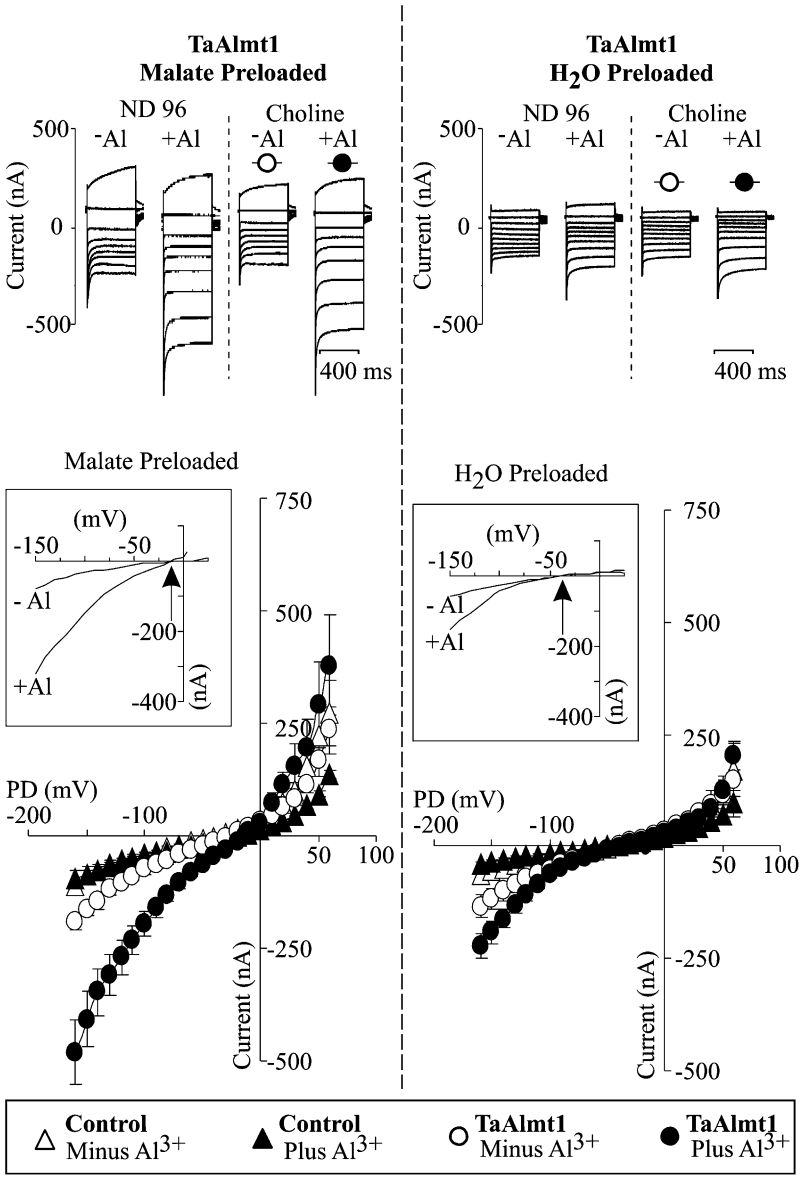


**Figure 5.** The TaALMT1 inward current does not cotransport $Na^+$. The top panel shows examples of families of currents from TaALMT1-expressing cells preloaded with malate (left) or water (right) in response to voltage pulses ranging from −140 to +60 mV (see "Materials and Methods" for detailed protocol). Currents were first recorded in ND96LA lacking or containing 100 $\mu$M $AlCl_3$ (10 $\mu$M $Al^{3+}$ activity). The bath solution was then changed to a solution in which NaCl was replaced by choline chloride (see Table I for detailed composition of the bath solution) lacking or containing $AlCl_3$ at an identical concentration as described above. The bottom panel shows the mean I/V relationships for TaALMT1 (circles) and control (triangles) cells preloaded with malate or water (as indicated at the top of the panel) recorded when the bath solution consisted of choline chloride in the absence (white symbols) or presence (black symbols) of 100 $\mu$M $AlCl_3$ in the bath solution. The inset for each set of I/V curves highlights the net inward TaALMT1-mediated current obtained after subtraction of the endogenous currents recorded in control cells bathed in solution of identical ionic composition. The arrows indicate the $E_{rev}$ ($n$ = 8).

(Fig. 7). As in the previous batch of cells, the outward currents recorded in TaALMT1-expressing cells were dominated by large, instantaneously activated currents, in contrast to the significantly smaller time-dependent currents recorded in control cells. As in previous recordings, the instantaneous nature of the TaALMT1-mediated outward currents was more evident at holding potentials more positive than +60 mV, at which the contribution (i.e. magnitude) of the TaALMT1-mediated currents became significantly larger relative to the endogenous time-dependent background currents. In both malate- and water-preloaded cells, lowering the $\{Cl^-\}_o$ resulted in a concentration-dependent reduction of the magnitude of the TaALMT1-mediated instantaneous outward current, while the magnitude of the inward currents remained relatively unchanged (Fig. 7A). In addition, the $E_{rev}$ of the TaALMT1-mediated currents in malate- or water-injected cells became more positive as the $\{Cl^-\}_o$ was lowered (Fig. 7, B and C). In contrast, although the reduction of $\{Cl^-\}_o$ also resulted in a decrease in the significantly smaller time-dependent endogenous outward current in control cells, it did not significantly alter the $E_{rev}$, as the $E_{rev}$ in control cells was relatively insensitive to the changes in $\{Cl^-\}_o$. The latter is consistent with *Xenopus* oocyte membrane potentials (i.e. control cells) being determined by the $Na^+/K^+$-ATPase and the permeability of the plasma membrane to $K^+$, with only minor contributions of $Na^+$ and $Cl^-$ conductance. The positive shift in the $E_{rev}$ recorded in TaALMT1-expressing cells as the $\{Cl^-\}_o$ was reduced (in both malate- and water-injected cells) is consistent with our previous findings suggesting that anion transport underlies TaALMT1-mediated currents.

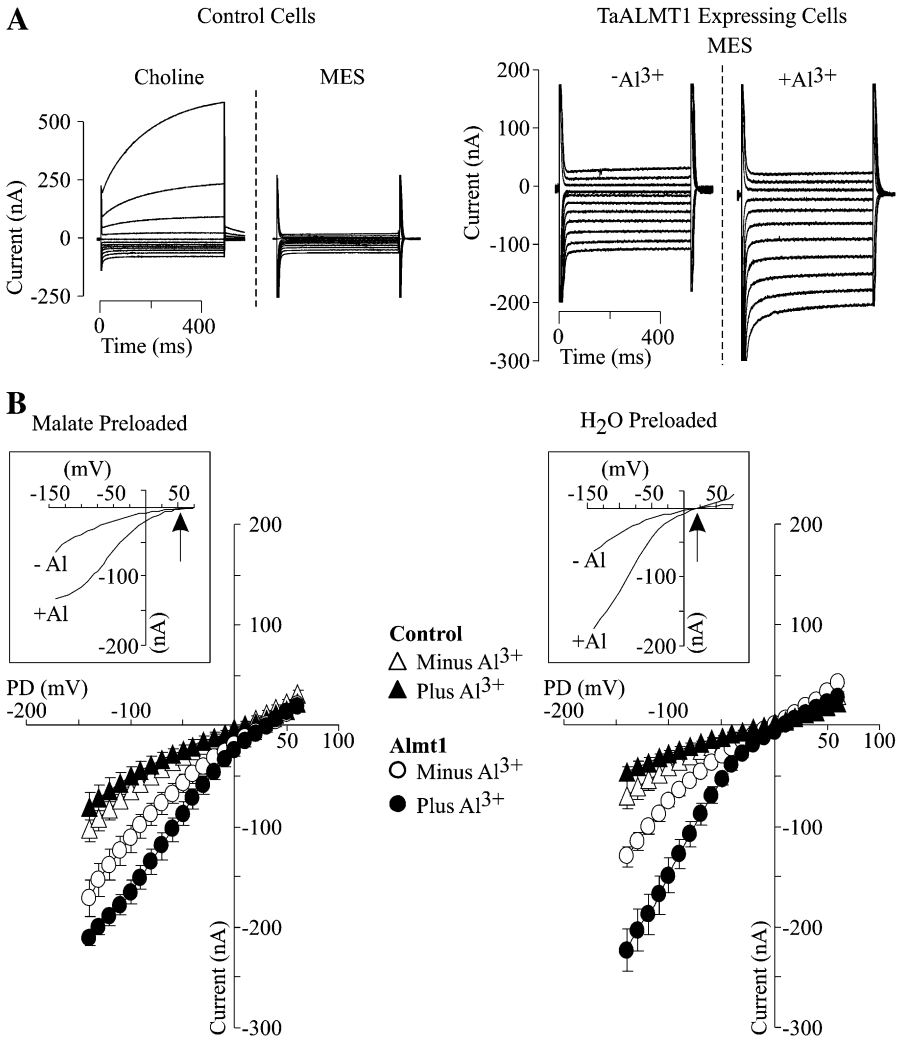


**Figure 6.** A, Examples of families of currents recorded from control (left) or TaALMT1-expressing (right) cells preloaded with malate and bathed in MES solution in response to voltage pulses ranging from −140 to +80 mV or −140 to +60 mV, respectively. Both types of cells were preloaded with malate. The left panel (control cells) compares endogenous currents obtained when the choline chloride bath solution was replaced with MES bath solution (see Table I). The right panel compares the TaALMT1 currents obtained in MES bath solution lacking (−) or containing (+) 100 $\mu$M $AlCl_3$. B, Mean I/V relationships for TaALMT1 (circles) and control (triangles) cells preloaded with malate (left) or water (right) recorded in MES bath solution prior to (white symbols) and following (black symbols) the addition of 100 $\mu$M $AlCl_3$ to the bath solution, obtained from recordings similar to those shown in A ($n$ = 6). The inset for each set of I/V curves highlights the magnitude and the $E_{rev}$ (arrow) of the net inward TaALMT1-mediated current obtained after subtraction of the endogenous currents recorded in control cells.

Figure 8 shows a detailed analysis of the biophysical properties obtained from the recordings shown in Figure 7. Increasing $\{Cl^-\}_o$ resulted in an increase in the conductance of the TaALMT1-mediated inward currents (i.e. anion efflux), with cells preloaded with malate showing consistently higher conductances than cells preloaded with water (Fig. 8A, left). These results are consistent with (1) an increase in the TaALMT1-mediated anion efflux rate (i.e. inward conductance) as the internal substrate (i.e. malate) increases and (2) $Cl^-$ permeation affecting the net TaALMT-mediated malate efflux. Increasing $\{Cl^-\}_o$ also resulted in an increase in the conductance of the TaALMT1-mediated outward currents (i.e. anion influx). However, unlike what was observed for the inward current, the outward current conductance of cells preloaded with malate was consistently lower that than in cells preloaded with water (Fig. 8A, right). These results indicate that (1) the TaALMT1-mediated anion influx (i.e. outward conductance) increases as the external anionic substrate ($Cl^-$) increases and (2) the permeability properties of the anion influx are also dependent on the nature of the ionic composition (i.e. not only $Cl^-$ but malate as well) of the intracellular compartment. In contrast, the conductance of the inward (and, to a lesser extent, outward) currents recorded from control cells (preloaded with malate or water) were relatively insensitive to changes in extracellular $Cl^-$ activity. Figure 8B shows the relationship between the $E_{rev}$ recorded from TaALMT1-expressing cells (preloaded with malate or water) at varying $\{Cl^-\}_o$ and the theoretical equilibrium potential for $Cl^-$ ($E_{Cl^-}$). Although at high $\{Cl^-\}_o$ the $E_{rev}$ values closely followed $E_{Cl^-}$, they deviated from $E_{Cl^-}$ as $\{Cl^-\}_o$ was reduced. The observation that $E_{rev}$ becomes less positive than $E_{Cl^-}$ as $\{Cl^-\}_o$ is reduced is consistent with the permeation of another anionic species (i.e. malate) contributing to the overall $E_{rev}$. Therefore, we proceeded to evaluate the "ability" of TaALMT1 to favor the transport of one anion over another. Commonly, the permeability ratio among two ions is calculated in bi-ionic conditions. However, since the exact intracellular anion composition of oocytes is unknown and cannot be entirely modified, we evaluated differences in the $E_{rev}$ that arise from changing $\{Cl^-\}_o$ to estimate

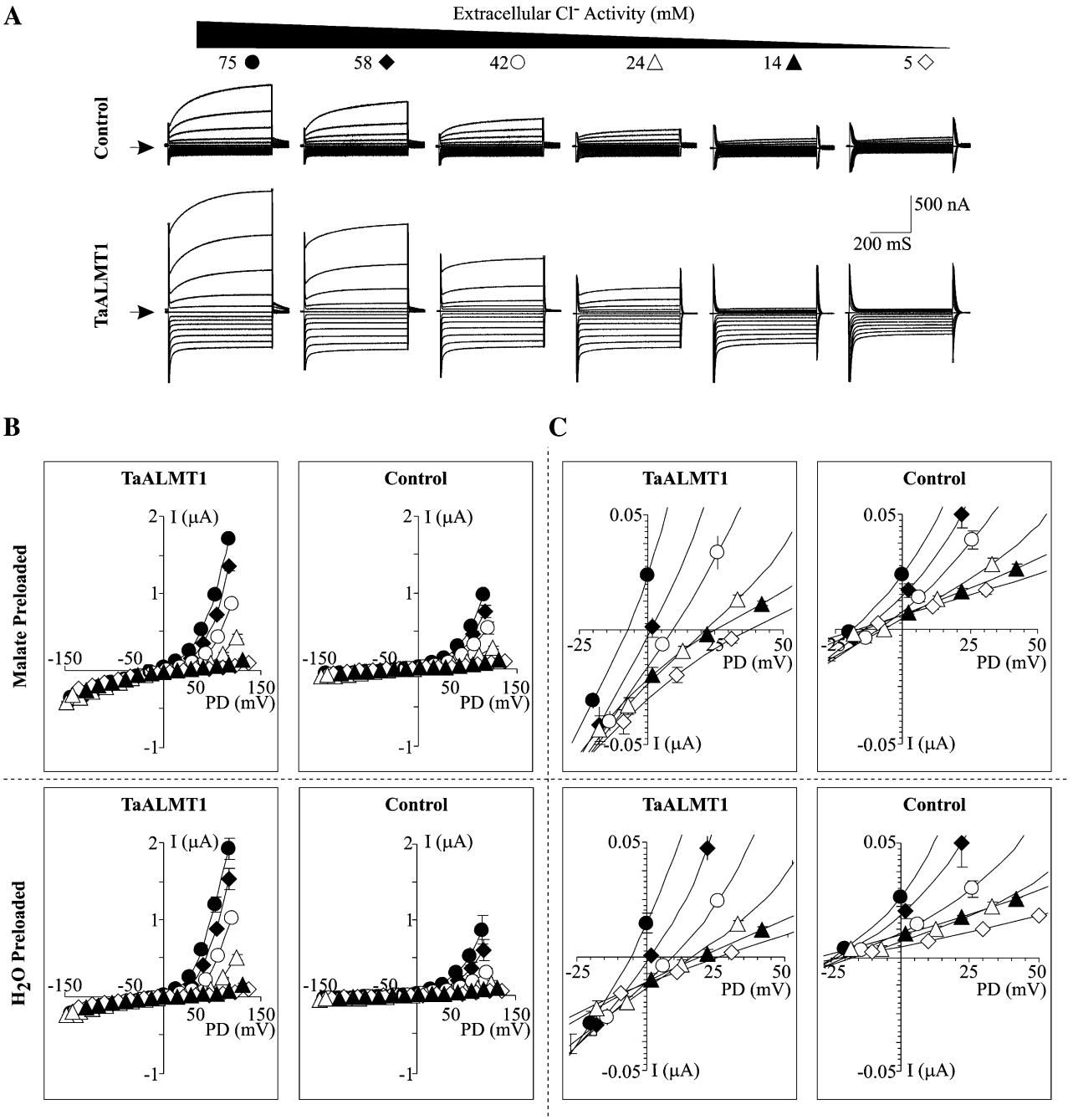


**Figure 7.** Anion selectivity of TaALMT1. A, Examples of control (top traces) and TaALMT1-mediated (bottom traces) currents recorded in response to voltage pulses ranging from −160 to +100 mV as the $\{Cl^-\}_o$ in the bath solution was varied to the value indicated at the top of each set of traces while maintaining the $Al^{3+}$ activity constant at 10 $\mu$M (see Table II). The arrow on the left margin indicates the zero current value. The current and time scales are detailed on the right margin. B, Mean I/V relationships for TaALTM1-expressing cells (left column) preloaded with malate (top row) or water (bottom row) from recordings like those described for A. The $\{Cl^-\}_o$ for each I/V curve corresponds to the symbol depicted at the top of each set of traces in A. The mean I/V relationships for control cells for each corresponding set of ionic conditions are shown in the right column ($n$ = 10). C, Range of potentials (−25 to +50 mV) from the I/V curves shown in B highlighting the $E_{rev}$. TaALMT1-expressing cells and control cells are shown in the left and right columns, respectively.

the permeability ratios between malate and chloride. Figure 8C shows the relationship between the observed shift in $E_{rev}$ relative to the $E_{rev}$ recorded at the highest $\{Cl^-\}_o$ and changes in $\{Cl^-\}_o$ as it is decreased in TaALMT1-expressing cells loaded with malate. This relationship could not be entirely explained by one fixed malate-to-$Cl^-$ permeability ratio ($P_{mal}{}^{2-}/P_{Cl}{}^-$) but rather by $P_{mal}{}^{2-}/P_{Cl}{}^-$ values that varied between

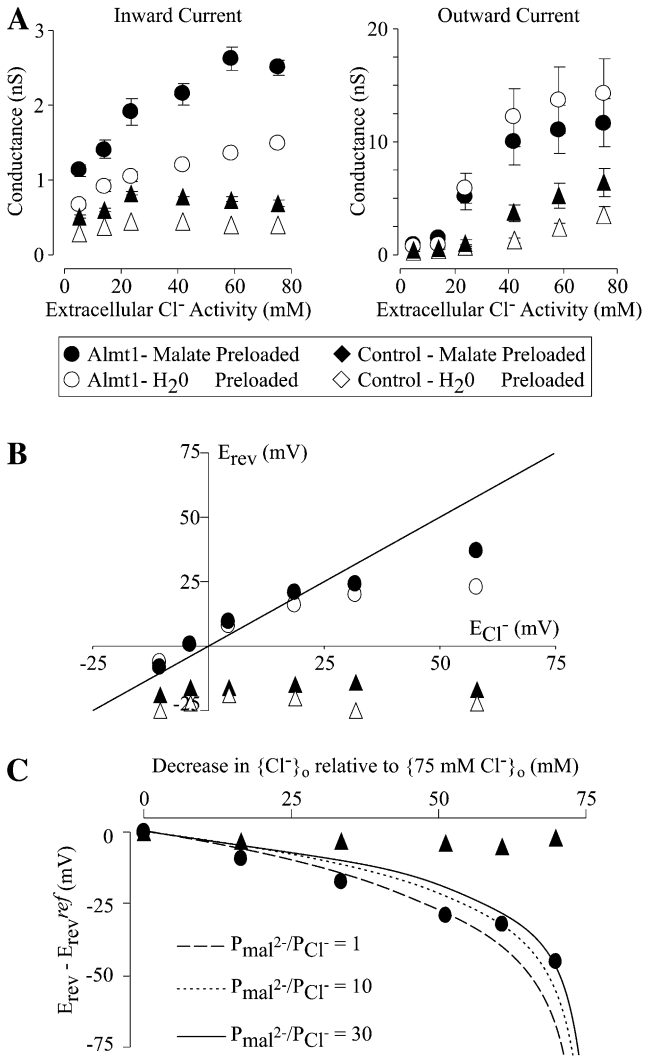


**Figure 8.** Conductivity and selectivity properties of the TaALMT1-mediated currents. A, Effect of $\{Cl^-\}_o$ on the conductance (G) of the inward (left) and outward (right) currents in TaALMT1-expressing (circles) and control (triangles) cells. The conductance was estimated by linear regression of the six most positive test potentials from the I/V relationships shown in Figure 7B. B, $E_{rev}$ from TaALMT1-expressing (circles) and control (triangles) cells preloaded with malate (black symbols) or water (white symbols), plotted as a function of the $E_{Cl^-}$, assuming an internal $Cl^-$ activity of 60 mM. $E_{rev}$ values correspond to those shown in Figure 7C. The line represents the theoretical values when $E_{Cl^-}$ equals $E_{rev}$. C, Shift in the observed $E_{rev}$ plotted as a function of the overall change in $\{Cl^-\}_o$. The shift in the observed $E_{rev}$ ($E_{rev} - E_{rev}^{ref}$) was defined as the difference between the recorded $E_{rev}$ at a given $\{Cl^-\}_o$ and the recorded $E_{rev}$ at the highest $\{Cl^-\}_o$ (i.e. $E_{rev}^{ref}$). Likewise, the decrease in $\{Cl^-\}_o$ was defined as the differences between the highest $\{Cl^-\}_o$ tested (i.e. 75 mM) and that present in the bath solution in each case. The lines represent the theoretical changes in $E_{rev}$ expected by decreasing $\{Cl^-\}_o$ at a given constant $P_{mal}^{2-}/P_{Cl^-}$ value (as indicated). The theoretical values were calculated from expected shifts in the net current (i.e. the sum of $I_{Cl^-}$ and $I_{mal}^{2-}$) predicted from the GHK current equation (Equation 14.5 in Hille, 2001), as $\{Cl^-\}_o$ varied and $\{Cl^-\}_i$ and $\{mal^{2-}\}_i$ remained constant at 60 and 4.5 mM, respectively.

1 and 30 depending on the magnitude of the reduction in $\{Cl^-\}_o$. The implications of these observations are addressed below (see "Discussion").

The permeability of TaALMT1 to other physiologically relevant anions was also evaluated by replacing the $Cl^-$ in the bath solution with $NO_3^-$ or $SO_4^{2-}$ (Fig. 9). Replacement of $Cl^-$ by either of these anions did not result in any significant changes in the outward currents (i.e. anion influx) recorded from control cells that were preloaded with malate or water. In contrast, TaALMT1-expressing cells showed a significant increase in the outward current conductivity when $Cl^-$ was substituted by $NO_3^-$. On the other hand, $Cl^-$ substitution by $SO_4^{2-}$ resulted in a modest decrease in the TaALMT1-mediated outward currents, suggesting a poor permeability for this divalent anion. The dependence of $NO_3^-$ conductivity on the intracellular malate concentration ($NO^{3-}$ conductivity being large in cells that were preloaded with water) was similar to that described for $Cl^-$ permeation (outward current; Fig. 8A). These observations are consistent with a deviation from the independence principle described above, in that it appears that an anion on one side of the oocyte plasma membrane influences the way a second anion behaves along the permeation pathway. Regardless of the mechanism of anion permeation, the overall results indicate that TaALMT1 has structural features that enable it to permeate a variety of anions, such as malate, $Cl^-$, $NO_3^-$, and, possibly, $SO_4^{2-}$ (to a lower extent).

## DISCUSSION

The growing genetic, biochemical, and functional evidence strongly indicates that TaALMT1 encodes the transporter mediating the Al-activated organic acid release that underlies the Al tolerance response in wheat roots. Likewise, the strong correlation between the functional and activation properties of $Al^{3+}$-activated anion channels (ALAACs) previously identified in protoplasts isolated from root tips of Al-tolerant wheat (Ryan et al., 1997; Zhang et al., 2001) and those described for TaALMT1 here suggests that this gene quite likely encodes the transporter that was studied in these wheat root protoplast studies. This novel type of transporter has also been identified in protoplasts isolated from root tips of Al-resistant maize (Kollmeier et al., 2001; Piñeros and Kochian, 2001; Piñeros et al., 2002), in which Al-activated root citrate exudation has been shown to play a key role in Al tolerance (however, see Piñeros et al., 2005). An increasing number of functionally expressed ALMT homologues (TaALMT, BnALMT1, AtALMT1, and ZmALMT1) are starting to emerge in the literature, providing some preliminary information regarding the functional characteristics of these transporters.

### Functional Inferences

#### *Activation by $Al^{3+}$*

When expressed in oocytes, the activity of TaALMT, BnALMT1, and AtALMT1 is dependent on the pres-

ence of extracellular $Al^{3+}$. In this study, we have established that although the activity of TaALMT1 is highly dependent on the presence of extracellular $Al^{3+}$, this transporter is not exclusively activated by extracellular $Al^{3+}$ (as proposed by Sasaki and coworkers [2004]) but, rather, its activity is "enhanced" by the presence of $Al^{3+}$. This observation is in agreement with the $Al^{3+}$ enhancement reported for AtALMT1 (Hoekenga et al., 2006) and indicates that at least these two ALMT transporters possess intrinsic properties that allow ion permeation in the absence of $Al^{3+}$. A thorough examination of BnALMT1 transport properties over a wider range of voltages is still required in order to establish whether this functional feature is common among other ALMTs. Although the exact process by which $Al^{3+}$ enhances ALMT-type transporter activity remains unknown, the functional data available at present provided by electrophysiological studies offer some insight regarding plausible mechanisms. Our study indicates that TaALMT1 has a high affinity (about 5 $\mu$M $Al^{3+}$ activity) for $Al^{3+}$. Furthermore, the lack of change in the $E_{rev}$ upon current enhancement by $Al^{3+}$ suggests that the binding process of $Al^{3+}$ to TaALMT1 does not alter its selectivity properties but solely increases its permeability. Such enhancement of transport activity is analogous to that described for other ligand-gated transporters; in our case, $Al^{3+}$ would be acting as an agonistic ligand. Thus, in the absence of $Al^{3+}$, ALMT-type transporters would spend a greater fraction of time in a closed state. Upon exposure, binding of $Al^{3+}$ to the transporter results in a conformational change that favors its open state, consequently increasing its transport activity and facilitating anion movement. This model is in agreement with patch-clamp studies characterizing ALAAC channels. For example, single channel recordings from excised patches from maize root tip protoplasts indicated that exposure to $Al^{3+}$ results in an increase in ALAAC channel activity (Piñeros and Kochian, 2001; Piñeros et al., 2002). Likewise, whole cell recordings have shown that ALAAC activity is strictly dependent on the presence of extracellular $Al^{3+}$, as removal of $Al^{3+}$ from the extracellular solution results in current inactivation (Ryan et al., 1997; Piñeros and Kochian, 2001; Zhang et al., 2001; Piñeros et al., 2002). Nonetheless, it is worth noting that not all ALMT-type transporters are likely to be regulated by the proposed agonistic ligand-gated mechanism. The large transport activity of the recently characterized ZmALMT1 (Piñeros et al., 2008) is relatively insensitive to the presence of $Al^{3+}$, suggesting that $Al^{3+}$ does not bind to this protein, binds with a lower affinity, or binds but does not promote any conformational changes in the transporter. These observations are also consistent with patch-clamp observations reported for other ALAACs identified in maize root protoplasts, in which removal of external $Al^{3+}$ did not result in channel inactivation (Kollmeier et al., 2001).

***Permeability and Selectivity***

Malate permeability for TaALMT1 and BnALMT was originally inferred from the observation that the $Al^{3+}$-enhanced inward ALMT-mediated currents were only present in those cells in which the internal malate concentration was increased to millimolar concentrations by preloading the cells with Na-malate. Likewise, it was originally presumed that the endogenous malate concentration in nonloaded cells (i.e. the absence of an external source of malate) was simply too low to generate any measurable ALMT-mediated currents. However, this study indicates that although smaller in magnitude, at sufficiently negative membrane potentials TaALMT1 also mediates $Al^{3+}$-enhanced inward currents in water-injected cells. Unfortunately, we were unable to establish the exact identity of the endogenous substrate that underlies the TaALMT1-mediated currents in this case. Nonetheless, the increase in intracellular malate was positively correlated with the increase in TaALMT1-mediated inward conductivity (i.e. transport), suggesting that TaALMT1 underlies the increase in permeability (i.e. malate transport). Furthermore, our results indicate a strong correlation between the increase in TaALMT1 conductivity and the shift in $E_{rev}$ as the intracellular malate activity increased. This correlation indicates that not only does malate permeate TaALMT1 but it does so in a selective manner. The remarkable similarity between the kinetics of the inward net TaALMT1 currents shown in Figure 1D and those described for the Al-activated malate-permeable channels recorded in wheat protoplasts (Ryan et al., 1997; Zhang et al., 2001) strongly suggests that the Al-activated currents recorded in wheat protoplasts are quite likely due to TaALMT1 transport activity. Interestingly, these patch-clamp studies did not report the presence of Al-activated outward currents in wheat protoplasts. In our study, we have demonstrated that TaALMT1 is capable of mediating outward currents (i.e. anion influx), provided that the extracellular anion concentration is large. As the electrochemical gradient becomes unfavorable for anion uptake (i.e. low extracellular concentration similar to that employed in the patch-clamp experiments), the magnitude of the outward currents is significantly reduced. Our results indicate that, under favorable ionic environments such as high extracellular anion concentration, TaALMT1 is not only permeable to malate but possibly can mediate a large influx of other physiologically relevant mineral anions (as inferred from the outward currents) such as $Cl^-$, $NO_3^-$, and $SO_4^{2-}$ (to a lesser extent). Nonetheless, further characterization of the nature of the TaALMT1-mediated outward currents is required to substantiate its potential physiological roles. Although we have established some of the preliminary permeability and selectivity characteristics for this anion influx pathway, the nature of our experimental system (i.e. expression in *Xenopus* oocytes) is prone to significant variability arising from

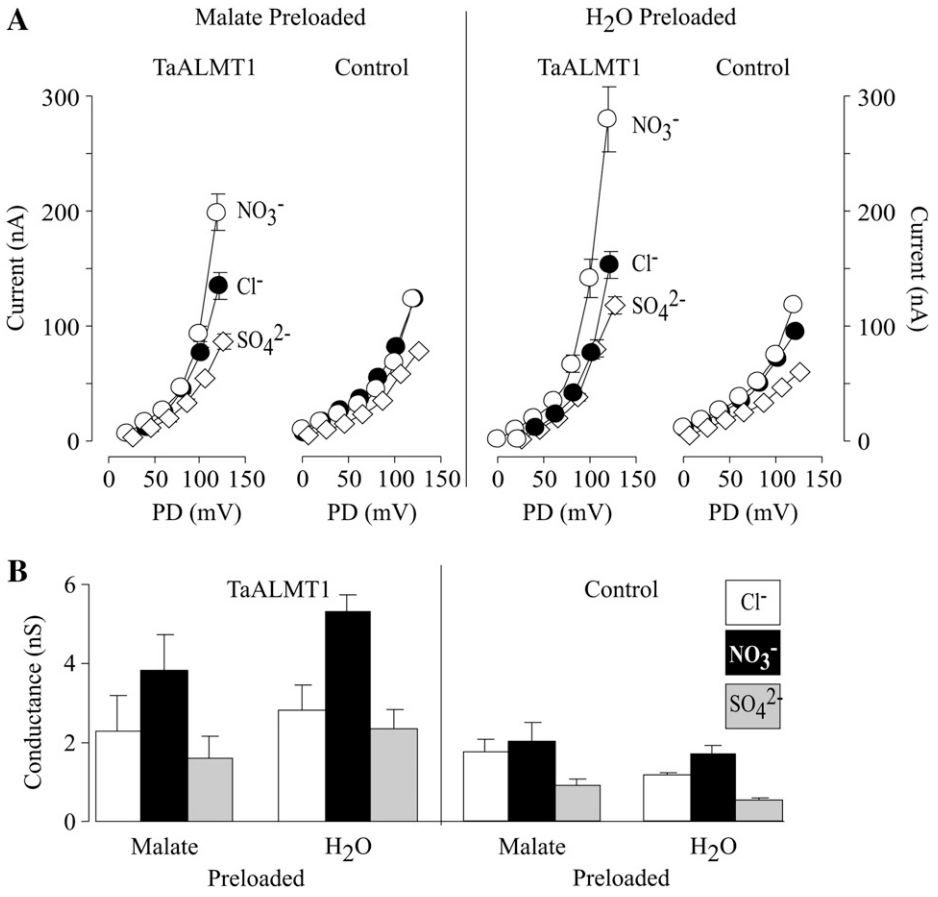


**Figure 9.** TaALMT1 permeability to other monovalent and divalent anions. A, Mean I/V relationships of the outward currents recorded from TaALMT1-expressing and control cells (preloaded with malate or water) bathed in a solution containing 9.6 mM $Cl^-$ (black circles), 9.6 mM $NO_3^-$ (white circles), or 9.6 mM $SO_4^{2-}$ (white diamonds). All solutions contained an additional 4.6 mM $Cl^-$ in the background (see "Materials and Methods" for ionic compositions; $n = 10$). B, Comparison of the outward current conductance recorded in TaALMT1-expressing and control cells (preloaded with malate or water) under the ionic conditions shown in A. The conductance was estimated by linear regression of the three most positive test potentials from the I/V relationships shown in A.

endogenous time-dependent outward currents, potentially obscuring some of its biophysical characteristics.

The permeability characteristics of TaALMT1 resemble those described for other plasma membrane anion channels in plant cells (see table 1 in Roberts, 2006), which are permeable to a variety of inorganic and organic anions but generally have a higher permeability for inorganic anions over organic anions. Although ALMTs are permeable to a variety of organic and inorganic anions, the net flux of a given anion will be determined not only by the electrochemical gradient but also by the selectivity of the transporter (i.e. its ability to discriminate between different ions). In that regard, the direction of the shift in $E_{rev}$ resulting from varying the intracellular and/or extracellular anionic activities is consistent with TaALMT1 being more selective for malate over other anions. Furthermore, the permeability ratios estimated in this study (as high as $P_{mal}^{2-}/P_{Cl}^{-} = 30$ at low extracellular $Cl^-$ activities) were significantly larger than those reported for any plasma membrane anion channels in plant cells (Roberts, 2006). In principle, this observation would indicate that at low extracellular $Cl^-$ activities, TaALMT1 is highly selective (about 30 times more) for malate relative to $Cl^-$. Nonetheless, the dependence of $P_{mal}^{2-}/P_{Cl}^{-}$ on the extracellular $Cl^-$ activity is indicative of deviations from the independence principle assumed in the Goldman-Hodgkin-Katz theory (Hille, 2001). Thus, since the constant field theory assumptions are unlikely to hold for the case of TaALMT1, the calculated $P_{mal}^{2-}/P_{Cl}^{-}$ can only be used as a guide to the relative affinity (i.e. selectivity) of TaALMT1 under this given set of ionic conditions. Consequently, a $P_{mal}^{2-}/P_{Cl}^{-}$ between 10 and 30 represents only an approximation of that expected under physiologically more relevant ionic concentrations. Although some preliminary evidence (based on the shift of $E_{rev}$ upon increasing intracellular malate) suggests that AtALMT1 is also more selective for malate than for $Cl^-$ (Hoekenga et al., 2006), a thorough examination of AtALMT1 as well as BnALMT1 under varying ionic conditions will be required to establish whether these two ALMT-type transporters share common permeability and selectivity features with TaALMT1. Interestingly, although the recently characterized ZmALMT1 is also permeable to $Cl^-$, $NO_3^-$, and $SO_4^{2-}$, it has weak permeability/selectivity for organic acids (Piñeros et al., 2008). Such a lack of selectivity relative to TaALMT1 is consistent with that described for ALAACs recorded in maize root protoplasts, which, although permeable to citrate and malate, poorly discriminated for these ions over other predominant anions such as $Cl^-$ (Kollmeier et al., 2001).

### Structural Inferences

Although the maize ZmALMT1 shares a high degree of sequence similarity/identity to other ALMT-type transporters functionally characterized to date, minor amino acid substitutions in the regulatory and permeation pathway domains of this protein must account for its lack of sensitivity to $Al^{3+}$ and different permeability/selectivity characteristics, respectively. Thus, it is tempting to speculate that minor differences in the primary structures of ALMT-type transporters can result in significant regulatory and functional (i.e. permeation/selectivity) differences, which in turn help determine their distinct roles in planta. Based on the existing primary structures and functional data available for ALMT-type proteins, some preliminary structural inferences can be made. Comparisons between the predicted secondary structures indicate that these proteins are structurally similar, with an N-terminal region consisting of five to six common membrane-spanning domains followed by a long hydrophilic C-terminal tail (see figure 4 in Piñeros et al., 2008). Amino acid sequence alignments indicate that these transporters share significant amino acid identity, with a higher degree of conservation over the N-terminal region relative to the more variable hydrophilic C-terminal region. By analogy with other well-characterized transporters, it is quite likely that the N-terminal region containing the membrane-spanning domains is responsible for forming the permeation pathway (i.e. pore structure) of the ALMT-type proteins. In contrast, the more variable hydrophilic C-terminal long tail is likely to be involved in the regulation of these transporters. In fact, this region is characterized by a number of motifs possibly involved in protein phosphorylation. Given that this region contains most of the variation among the sequences, it is tempting to propose that differences in regulatory mechanisms (such as the presence or absence of specific amino acid residues that bind $Al^{3+}$), which grant ALMT transporters different in planta roles, may exist within this region.

In this study, we have thoroughly characterized the biophysical and functional properties of TaALMT1 with the goal of providing a platform for future functional-structural analyses of this family of transporters. Studies involving established molecular biology techniques in combination with functional analysis by electrophysiological means should prove very useful in the elucidation of the domains, and ultimately the amino acid residues underlying the regulatory (e.g. $Al^{3+}$ enhancement) and functional (e.g. permeability/selectivity) mechanisms, in this new family of ion transporters.

## MATERIALS AND METHODS

### In Vitro Transcription and Complementary RNA Injection

The coding region of *TaAlmt1-1* (previously referred to as Almt1-1) from wheat (*Triticum aestivum*) was cloned between the 3′ and 5′ untranslated regions of a *Xenopus laevis* β-globin gene of the T7TS plasmid. Two types of constructs were used to test for RNA stability. The first type contained only the coding region of TaALMT1, while the second contained a kosak consensus (GCCGCCACC) immediately upstream of the initiation codon. Complementary RNA (cRNA) was prepared from the linearized (*Sca*I) plasmid DNA templates using the RNA Capping Kit (Stratagene) following the manufacturer's instructions. The cRNA was divided into 1.5-μL aliquots and stored at −80°C until injection. Harvesting of stage V to VI *Xenopus* oocytes was performed as described by Golding (1992). Defolliculated oocytes were maintained in ND88 solution (supplemented with 50 μg $mL^{-1}$ gentamycin) overnight prior to injections. *Xenopus* oocytes were injected with 48 nL of water containing 40 ng of cRNA encoding *TaALMT1* (or 48 nL of water as a control) and incubated in ND88 at 18°C for 2 to 4 d.

### Electrophysiological Recordings and Bath Solutions

Whole cell currents were recorded under constant perfusion at room temperature (22°C) with a GeneClamp 500 amplifier (Axon Instruments) using conventional two-electrode voltage clamp techniques. The output signal was digitized and analyzed using a Digidata 1320A-PClamp 9 data acquisition system (Axon Instruments). Recording electrodes filled with 0.5 M $K_2SO_4$ and 30 mM KCl had resistances between 0.5 and 1.2 MΩ. Recordings were performed in both control oocytes and *TaALMT1*-expressing oocytes that were preloaded or not with malate or water at 2 h prior to the recording. Preloading was achieved by injecting each cell with 48 nL of 0.1 M sodium malate. Electrophysiological recordings indicated that the insertion of a kosak motif did not change the properties or the magnitude of expression of TaALMT1 in oocytes. Recordings were performed in various types of bath solutions. The composition of the ND88 recording solution was identical to that described by Sasaki et al. (2004). The basic ND96 solution consisted of 96 mM NaCl, 1 mM KCl, and 1.8 mM $CaCl_2$ adjusted to pH 4.5. When present, $Al^{3+}$ was added as $AlCl_3$ to final concentrations of 25, 50, 100, and 200 μM, yielding $Al^{3+}$ activities of 2.5, 5, 10, and 19 μM, respectively. The remaining bath solutions derived from this ionic composition are described in Tables I and II. The solutions used to test nitrate or sulfate permeation consisted of a solution containing 1 mM KCl, 1.8 mM $CaCl_2$, and 9.6 mM NaCl, $NaNO_3$, or $Na_2SO_4$. The ionic activities were estimated using GEOCHEM-PC (Parker et al., 1995).

### Voltage Protocols and Data Analysis

Steady-state currents were measured in response to voltage pulses (400 or 500 ms in duration) between −160 or −140 and +60 or +100 mV (in 10- or 20-mV increments). The specific range of voltage pulses is detailed in each figure legend. A 10-s resting interval at 0 mV was allowed between successive voltage increments. For clarity, in figures illustrating examples of current recordings, only currents in response to 20-mV steps are shown. Potentially, I/V relationships constructed by measuring the current amplitude at the beginning of the trace could minimize the contribution of the variable endogenous time-dependent currents observed at positive potentials and, consequently, more accurately reflect the instantaneous nature of the TaALMT1-mediated outward current. However, given the partial deactivation of the TaALMT1-mediated inward currents, we opted to construct I/V relationships by measuring the steady-state current amplitude at the end of each voltage pulse. The data presented were collected using cells from eight different donor frogs. Rather than normalizing the current magnitudes throughout the study, we measured the electrogenic activity of each batch of control cells for each ionic condition. This allowed us to compare TaALMT1-expressing and control cells within each data set (i.e. I/V relationship obtained in one given batch of cells under the same set of ionic conditions). Thus, we present the raw data for both TaALMT1-expressing and control cells, rather than subtracting the endogenous currents from the TaALMT1 current traces. The latter allows the reader to assess the degree of contribution from the endogenous currents in different batches of cells, rather than potentially misleading the reader by presenting only the findings after subtraction of the endogenous currents. The values shown in the I/V relationships represent the average of at least *n* different cells as indicated in each figure legend, and error bars denote SE. PD in all figures showing I/V relationships stands for the potential difference established during the holding or test potential. Liquid junction potentials were measured and corrected according to the method of Neher (1992). All potentials shown (including $E_{rev}$) have been corrected by offline subtraction of the experimental junction potentials tested for each ionic condition.

## Intracellular Malate Determinations

Malate preloading (i.e. injecting each cell with 48 nL of 0.1 M sodium malate) theoretically results in an increase of 9.1 to 9.4 mM in the intracellular Na-malate concentration. The latter calculation assumes a cell diameter between 1.0 and 1.2 mm for stage V and VI oocytes as well as the fact that the 48 nL injected is retained in the oocyte. To verify these predictions, we determined the internal malate concentration in preloaded and nonpreloaded oocytes. Oocytes (12 cells per replica) were disrupted in 200 $\mu$L of water in a microfuge tube and spun for 4 min at 10,000 rpm at 4°C. The " extraction supernatant" was recovered, avoiding the lipid top layer, and spun again. Excess $Cl^-$ was removed using resin from an OnGuard-Ag chromatography column (Dionex). Half of the extraction supernatant was used to saturate 20 mg of resin by mixing. The resin was spun for 1 min, and the supernatant was discarded. The saturated resin was mixed with the remaining extraction supernatant, mixed, and briefly spun. The resulting supernatant was recovered and used for capillary electrophoresis analysis. Organic acid determinations were performed using a P/ACE 5510 CE system (Beckman Instruments) under the conditions described previously (Piñeros et al., 2002). The identity of the peaks was verified by spiking the samples with known standards. Internal malate concentrations calculated from nonloaded oocytes ranged between 200 and 400 $\mu$M. Internal malate concentration in malate-preloaded cells was in the range of 8.2 $\pm$ 0.2 mM. As this intracellular malate concentration was close to that predicted theoretically, the value determined experimentally was used for the permeability ratio determinations. GEOCHEM-PC predicted that at relatively neutral cytoplasmic pH (i.e. pH 7.2), 99.5% of the malate injected as Na-malate will be found as free ligand, with free ionic activity (i.e. $\{mal^{2-}\}_i$) of 4.5 mM.

## ACKNOWLEDGMENT

We thank Dr. Lyza Maron for critical reading of the manuscript.

Received March 24, 2008; accepted June 1, 2008; published June 11, 2008.

## LITERATURE CITED

**Delhaize E, Craig S, Beaton CD, Bennet RJ, Jagadish VC, Randall PJ** (1993a) Aluminum tolerance in wheat (*Triticum aestivum* L.). 1. Uptake and distribution of aluminum in root apices. Plant Physiol **103:** 685–693

**Delhaize E, Gruber BD, Ryan PR** (2007) The roles of organic anion permeases in aluminium resistance and mineral nutrition. FEBS Lett **581:** 2255–2262

**Delhaize E, Ryan PR, Hebb DM, Yamamoto Y, Sasaki T, Matsumoto H** (2004) Engineering high-level aluminum tolerance in barley with the ALMT1 gene. Proc Natl Acad Sci USA **101:** 15249–15254

**Delhaize E, Ryan PR, Randall PJ** (1993b) Aluminum tolerance in wheat (*Triticum aestivum* L.). 2. Aluminum-stimulated excretion of malic acid from root apices. Plant Physiol **103:** 695–702

**Golding A** (1992) Maintenance of Xenopus laevis and oocyte injection. Methods Enzymol **207:** 266–279

**Hille B** (2001) Ion Channels of Excitable Membranes. Sinauer Associates, Sunderland, MA

**Hoekenga OA, Maron LG, Piñeros MA, Cancado GMA, Shaff J, Kobayashi Y, Ryan PR, Dong B, Delhaize E, Sasaki T, et al** (2006) AtALMT1, which encodes a malate transporter, is identified as one of several genes critical for aluminum tolerance in Arabidopsis. Proc Natl Acad Sci USA **103:** 9738–9743

**Kochian LV, Hoekenga OA, Piñeros MA** (2004) How do crop plants tolerate acid soils? Mechanisms of aluminum tolerance and phosphorous efficiency. Annu Rev Plant Biol **55:** 459–493

**Kochian LV, Piñeros MA, Hoekenga OA** (2005) The physiology, genetics and molecular biology of plant aluminum resistance and toxicity. Plant Soil **274:** 175–195

**Kollmeier M, Dietrich P, Bauer CS, Horst WJ, Hedrich R** (2001) Aluminum activates a citrate-permeable anion channel in the aluminum-sensitive zone of the maize root apex: a comparison between an aluminum-sensitive and an aluminum-resistant cultivar. Plant Physiol **126:** 397–410

**Kovermann P, Meyer S, Hörtensteiner S, Picco C, Scholz-Starke J, Ravera S, Lee Y, Martinoia E** (2007) The Arabidopsis vacuolar malate channel is a member of the ALMT family. Plant J **52:** 1169–1180

**Ligaba A, Katsuhara M, Ryan PR, Shibasaka M, Matsumoto M** (2006) The BnALMT1 and BnALMT2 genes from *Brassica napus* L. encode aluminum-activated malate transporters that enhance the aluminum resistance of plant cells. Plant Physiol **142:** 1294–1303

**Magalhaes JV, Liu J, Guimaraes CT, Lana UGP, Alves VMC, Wang YH, Schaffert RE, Hoekenga OA, Pineros MA, Shaff JE, et al** (2007) A gene in the multidrug and toxic compound extrusion (MATE) family confers aluminum tolerance in sorghum. Nat Genet **39:** 1156–1161

**Mitcheson JS, Chen J, Sanguinetti MC** (2000) Trapping of a methanesulfonanilide by closure of the HERG potassium channel activation gate. J Gen Physiol **115:** 229–240

**Neher E** (1992) Correction for liquid junction potentials in patch clamp experiments. Methods Enzymol **207:** 123–131

**Parker DR, Norvell WA, Chaney RL** (1995) GEOCHEM-PC: a chemical speciation program for IBM and compatible computers. *In* RH Loeppert, AP Schwab, S Goldberg, eds, Chemical Equilibrium and Reaction Models. Soil Science Society of America, Madison, WI, pp 253–269

**Piñeros MA, Cançado GMA, Maron LG, Lyi SM, Menossi M, Kochian LV** (2008) Not all ALMT1-type transporters mediate aluminum-activated organic acid responses: the case of *ZmALMT1*—an anion selective transporter. Plant J **53:** 352–367

**Piñeros MA, Kochian LV** (2001) A patch-clamp study on the physiology of aluminum toxicity and aluminum tolerance in maize: identification and characterization of $Al^{3+}$-induced anion channels. Plant Physiol **125:** 292–305

**Piñeros MA, Magalhaes JV, Carvalho Alves VM, Kochian LV** (2002) The physiology and biophysics of an aluminum tolerance mechanism based on root citrate exudation in maize. Plant Physiol **129:** 1194–1206

**Piñeros MA, Shaff JE, Manslank HS, Alves VMC, Kochian LV** (2005) Aluminum resistance in maize cannot be solely explained by root organic acid exudation: a comparative physiological study. Plant Physiol **137:** 231–241

**Raman H, Zhang KR, Cakir M, Appels R, Garvin DF, Maron LG, Kochian LV, Moroni JS, Raman R, Imtiaz M, et al** (2005) Molecular characterization and mapping of ALMT1, the aluminium-tolerance gene of bread wheat (Triticum aestivum L.). Genome **48:** 781–791

**Roberts SK** (2006) Plasma membrane anion channels in higher plants and their putative functions in roots. New Phytol **169:** 647–666

**Ryan PR, Skerrett M, Findlay GP, Delhaize E, Tyerman SD** (1997) Aluminum activates an anion channel in the apical cells of wheat roots. Proc Natl Acad Sci USA **94:** 6547–6552

**Sasaki T, Yamamoto Y, Ezaki B, Katsuhara M, Ahn SJ, Ryan PR, Delhaize E, Matsumoto H** (2004) A wheat gene encoding an aluminum-activated malate transporter. Plant J **37:** 645–653

**Weber WM** (1999) Endogenous ion channels in oocytes of Xenopus laevis: recent developments. J Membr Biol **170:** 1–12

**Yamaguchi M, Sasaki T, Sivaguru M, Yamamoto Y, Osawa H, Ahn SJ, Matsumoto H** (2005) Evidence for the plasma membrane localization of Al-activated malate transporter (ALMT1). Plant Cell Physiol **46:** 812–816

**Zhang WH, Ryan PR, Tyerman SD** (2001) Malate-permeable channels and cation channels activated by aluminum in the apical cells of wheat roots. Plant Physiol **125:** 1459–1472